Surrogate modeling and control optimization of batch crystallization process of β form LGA

Bo Song [a,b], Tao Liu [a,b,*], Mingyan Zhao [a,b], Yan Cui [a,b], Yuanjun Li [a,b]

a Key Laboratory of Intelligent Control and Optimization for Industrial Equipment of Ministry of Education, Dalian University of Technology, Dalian 116024, P. R. China (e-mail: tliu@dlut.edu.cn)
b Institute of Advanced Control Technology, Dalian University of Technology, Dalian 116024, P. R. China

Abstract: To describe a quantitative relationship between the operating conditions of cooling crystallization process and product crystal size distribution (CSD), a surrogate modelling method based on the Gaussian process regression (GPR) is proposed by using only experimental data of batch crystallization process of β form L-glutamic acid (LGA). A modified design of experiments (DoE) is presented to reduce the number of batch crystallization experiments. Based on the surrogate model, an objective function reflecting the concentration of product CSD and desired yield is introduced to optimize these operating conditions. Experiments on the seeded cooling crystallization process of β-LGA are conducted to verify the effectiveness and advantage of the proposed method.

Keywords: Batch crystallization process, surrogate modelling, crystal size distribution, Gaussian regression model, process optimization.

1. INTRODUCTION

Batch crystallization technology has been widely applied in pharmaceutical industry and fine chemistry, owing to its advantage for yielding crystal products with a specific size range (Nagy et al,, 2013). For batch optimization of cooling crystallization processes, the existing references were mainly dependent on the crystal growth kinetic model involved with crystal aggregation, breakage and agglomeration for process design and optimization. For instance, a size-dependent kinetic model was used to design the optimal cooling operation for a seeded cooling crystallization process of anticancer drugs (Seki & Su, 2015). Alternative population balance models (PBMs) were also explored for the optimal design of solution supersaturation during crystallization (Khan et al., 2011). In fact, it remains open as yet to simultaneously optimize the temperature and supersaturation profile for obtaining the desired product yield and CSD, based on the above process kinetic models. The developed multi-objective optimization methods (Hemalatha & Rani, 2017) were primarily devoted to improve product yield and productivity.

Since the developed PBMs are generally of partial-differential equation and computationally demanding for numerical solution of CSD, surrogate modeling has been increasingly explored in the recent years (Zhong et al., 2019), based on approximating the process output response rather than the process kinetic mechanism. A modified polynomial chaos expansion (PCE) based surrogate modeling method was presented to design the optimal temperature profile for obtaining desirable product yield of batch cooling crystallization (Sanzida & Nagy, 2014). Another surrogate modeling method (Busschaert & Waldherr, 2022) was developed to infer the crystal growth rate of aspirin during cooling crystallization, by using the Gaussian kernel functions for model building. Nevertheless, a considerable number of experiments need to be carried out to generate sufficient process data for such surrogate modeling, since the data-driven modeling approach depends on the design of experiments (DoE) for obtaining informative batch run data. Only a small number of references addressed DoE for modeling and optimization of cooling crystallization processes, although it has been utilized in various engineering fields (Ljungberg et al., 2023).

In this study, a novel surrogate modeling method is proposed to describe the nonlinear relationship between the operating conditions of crystallization process and product CSD, based on the Gaussian process regression (GPR). A sensitivity based DoE (herein named SDoE) is developed to save the number of batch experiments for acquiring informative crystallization process data, which adopts the information entropy of product CSD to evaluate its sensitivity with respect to the process operating conditions. Based on the GPR model, a comprehensive quality criterion is introduced to optimize the process operating conditions, which takes into account the information entropy of product CSD together with the desired product yield and size range. Experiments on the seeded cooling crystallization process of β form LGA are conducted to verify the effectiveness of the proposed modeling and optimization method.

2. PROBLEM DESCRIPTION

Since the spontaneous nucleation could be neglected in a seeded cooling crystallization process owing to the use of crystal seeds, a one-dimensional PBE for describing the crystal growth kinetics of a seeded cooling crystallization process is generally in the form of

$$\frac{\partial f_n(L,t)}{\partial t}+\frac{\partial (G(S,L)f_n(L,t))}{\partial L}=B(\theta_b,t)\delta(L-L_b) \quad (1)$$

where $f_n(L,t)$ denotes the crystal number density function in a size range of L, t the time, $G(S,L)$ the crystal

growth rate, $B(\theta_b,t)$ the nucleation rate, L_b the characteristic size of nuclei, and $\delta(L-L_b)$ the Dirac delta function. With the seeding operation, the initial process conditions are expressed by

$$\begin{cases} f_n(L,0)=f_{seed}(L) \\ f_n(0,t)=\dfrac{B(\theta_b,t)}{G(S,\theta_g)} \end{cases} \tag{2}$$

The crystal growth kinetics during crystallization is typically modeled by a power-law rate equation,

$$G(S,L)=k_{g,1}S^{k_{g,2}}(1+k_{g,3}L)^{k_{g,4}} \tag{3}$$

where $S=C(t)-C^*(t)$ is the absolute supersaturation, C the solute concentration, and $C^*=\alpha_1T^2+\alpha_2T+\alpha_3$ the solution solubility; Denote by α_1, α_2, α_3 the solubility coefficients, and by T the solution temperature; L denotes the one-dimensional crystal size. The kinetic model parameters are denoted by $\theta_g=[k_{g,1},k_{g,2},k_{g,3},k_{g,4}]$.

Since the secondary nucleation has been well utilized in industrial seeded crystallization processes, it is regarded as the dominant behavior of crystal nucleation, as described by a function between the relative supersaturation and volume of all crystals (Hermanto et al., 2008),

$$B(\theta_b,t)=k_b(S_r-1)\mu_3(t) \tag{4}$$

where k_b denotes the kinetic nucleation parameter, $S_r=C/C*$ is the supersaturation ratio and $\mu_3(t)$ is the third order moment of CSD defined by

$$\mu_k(t)=\int_0^\infty f_n(L,t)L^k dL\approx\sum_{i=1}^{N_q}w_i(t)L_i^k(t)\quad k=0,...,3 \tag{5}$$

where w_i denotes the corresponding weights and L_i is the length coordinate, which could be solved by using the product-difference (PD) algorithm (Gimbun et al., 2009); N_q indicates the number of discretized points with regard to the crystal size range for evaluation. It should be noted that μ_0, μ_1, μ_2, μ_3 are related to the normalized number of crystals within per unit volume, the averaged crystal length, averaged surface area of crystals, averaged crystal volume (or mass), respectively. To estimate the mass of solute consumed by crystal growth and the birth of nuclei during cooling crystallization, the mass balance equation is expressed by

$$\frac{dC(t)}{dt}=-3\rho_c k_v\left[G(S,L)\mu_3(t)+B(\theta_b,t)L_b^3\right] \tag{6}$$

where ρ_c is the solute density, and k_v is the volume shape factor.

Because CSD could not be analytically solved from the above PBE in Eq.(1), the high resolution finite volume method (HRFVM) (Gunawan et al., 2004; Simone et al., 2017) was developed to solve this kind of hyperbolic partial differential equation and applied for reconstructing CSD (Aamir et al., 2009). By discretizing the space domain, the HRFVM sets up a series of grid cells, where each grid point is specified by

$$\zeta_l(t)=\frac{1}{h_l}\int_{(l-1)h_l}^{lh_l}f_n(L,t)\mathrm{dL} \tag{7}$$

where ζ_l denotes the approximate number density in the l-th grid cell, h_l the size of the l-th grid cell.

From the above review on the existing PBM and HRFVM methods, it is obvious that the product CSD of cooling crystallization could not be explicitly solved or precisely predicted with regard to the process operating conditions like the cooling temperature profile and solution supersaturation. Hence, it is motivated to establish a surrogate model to describe the mapping relationship between the above operating conditions and product CSD, based on only the batch data of cooling crystallization. To save the number of experiments for such data-driven modeling, an SDoE method is proposed for practical application. Based on the established mapping model, these operating conditions are optimized for batch run, by introducing a comprehensive quality criterion related to the information entropy of product CSD and desired product yield for process optimization. These contents are presented in the following sections, respectively.

3. SURROGATE MODELLING

3.1 Sensitivity based design of experiments (SDoE)

To generate informative batch run data for surrogate modeling of the relationship between the process operating conditions and product CSD, while reducing the number of batch run experiments as much as possible, it is proposed to evaluate the sensitivity of product CSD with regard to the operating conditions, based on a few experiments under specified operating conditions in the permitted range.

Note that the concentration degree of product CSD by seeded cooling crystallization could be evaluated by the information entropy defined by

$$\Omega(\boldsymbol{o})=-\sum_{n_k=1}^{N_K}\zeta(\boldsymbol{o},y_{n_k})\log(\zeta(\boldsymbol{o},y_{n_k})) \tag{8}$$

where $\boldsymbol{o}$ denotes the operating conditions of solution supersaturation (SS) and cooling rate (CR), y_{n_k} the n_k-th product crystal size, and $\zeta(\boldsymbol{o},y_{n_k})$ denotes CSD with respect to the operating conditions.

To save the computational effort for estimating the traditional sensitivity indices, an estimation algorithm (Saltelli et al., 2010) is adopted to estimate first-order sensitivity indices $S_{\boldsymbol{o}}$ and total-order sensitivity indices $TS_{\boldsymbol{o}}$, i.e.,

$$S_{\boldsymbol{o}_{(i)}}=\frac{\frac{1}{N_S}\sum_{j=1}^{N_S}\Omega(\boldsymbol{o}_B)_j[\Omega(\boldsymbol{o}_{A\boldsymbol{o}_B}^{(i)})_j-\Omega(\boldsymbol{o}_A)_j]}{V(\Omega)} \tag{9}$$

$$TS_{\boldsymbol{o}_{(i)}}=\frac{\frac{1}{2N_S}\sum_{j=1}^{N_S}[\Omega(\boldsymbol{o}_A)_j-\Omega(\boldsymbol{o}_{A\boldsymbol{o}_B}^{(i)})_j]^2}{V(\Omega)} \tag{10}$$

where $\boldsymbol{o}_A$ and $\boldsymbol{o}_B$ are two independent sampling matrix of operating conditions with the dimension of $[N_S,N_O]$; the superscript $i=1,\ldots,N_O$ indicates the number of operating conditions; $\boldsymbol{o}_{A\boldsymbol{o}_B}^{(i)}$ is a matrix where all columns come from $\boldsymbol{o}_A$ except for the i-th column from $\boldsymbol{o}_B$.

Accordingly, the interaction sensitivity index between the

operating conditions of CR and SS is defined by

$$S_{CR,SS} = \sum_{i=1}^{N_O} [TS_{o(i)} - S_{o(i)}] \tag{11}$$

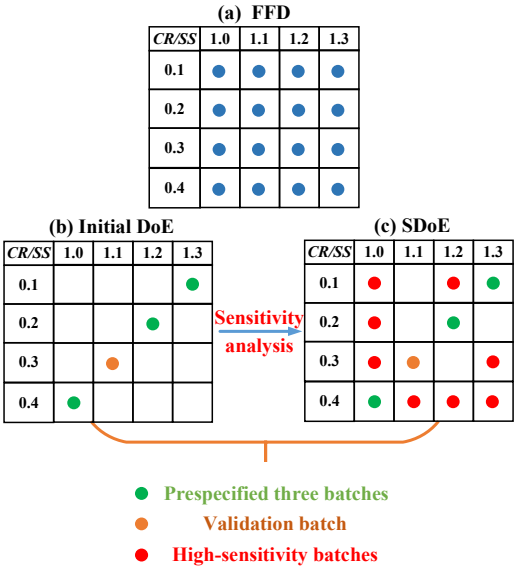

Figure 1. DoE with 2-factor and 4-level: (a) FFD; (b) Initial DoE; (c) SDoE

To reduce the number of factors and their levels by the commonly used full factorial design (FFD) (Montgomery, 2017) as shown in Figure 1 (a) in order to facilitate practical application, a sensitivity-based DoE (SDoE) approach is therefore proposed for designing α -factor and β -level (denoted by α^{β}) experiments. In the DoE, the operating conditions could be encoded in a range of [0,1] by normalization. For clarity, $\alpha = 2$ and $\beta = 4$ (2^4) are selected in this study, corresponding to CR with the levels of $[0.1, 0.2, 0.3, 0.4]$ and SS with the levels of $[1.0, 1.1, 1.2, 1.3]$, both of which are encoded by $[0, 0.33, 0.66, 1]$, respectively. Considering that experiments for model building should be conducted within a permitted range of the operating conditions, a few specific experiments with the number of $\lfloor \alpha^{\beta} / \beta \rfloor = 2^4 / 4 = 4$, including the boundary, main or sub diagonal points, are initially chosen for model building and sensitivity analysis, as shown in Figure 1 (b), so as to reduce the total number of experiments (i.e., α^{β}) required by FFD for parameter estimation.

3.2 Surrogate modeling by GPR

Based on the batch crystallization process data, a surrogate model is established herein by the GPR approach, for describing the nonlinear relationship between product CSD and the operating conditions of initial supersaturation and cooling rate. A GPR model is generally defined by a linear combination of N kernel functions (Deringer et al., 2021)

$$\tilde{\zeta}(\mathbf{L}) = \sum_{n=1}^{N} w_n k(\mathbf{L}, \mathbf{L}_n) \tag{12}$$

where $k(\mathbf{L}, \mathbf{L}_n)$ denotes a kernel function, $\mathbf{L}$ the lengths of crystals, $\mathbf{L}_n$ the characteristic lengths of crystals, and w_n the related weights; $\tilde{\zeta}(\mathbf{L})$ is used to approximate the product CSD with respect to the characteristic lengths of crystals.

Considering the complex dynamics of seeded cooling crystallization processes, it is important to take appropriate kernel functions to build up the GPR model for reflecting the mapping relationship between these operating conditions and product CSD. The Matérn (MT) kernel function (Williams & Rasmussen, 2006) is therefore adopted owing to its bimodal distribution for versatile approximation, expressed by

$$k_{\mathrm{MT}}(\mathbf{L}, \mathbf{L}_n) = \sigma_{\mathrm{M}}^2 \left(1 + \frac{\sqrt{3(\mathbf{L} - \mathbf{L}_n)}}{\ell_{\mathrm{M}}}\right) \exp\left(-\frac{\sqrt{3(\mathbf{L} - \mathbf{L}_n)}}{\ell_{\mathrm{M}}}\right) \tag{13}$$

where ℓ_{M}, σ_{M} and σ_{ε} are three hyperparameters referred to the characteristic width of kernel, variance of kernel, and the fitting residual. To overcome the issue that hyperparameter optimization through the traditional maximum likelihood estimation method likely fall into local minimum, a global optimization algorithm called BWO (Zhong et al., 2022) is adopted herein for searching out the optimal hyperparameter setting.

Hence, the above hyperparameters are optimized by the following minimization program,

$$\begin{aligned} \min_{hp} \ & RMSE = \sqrt{\frac{1}{N_{\mathrm{p}}} \sum_{i=1}^{N_{\mathrm{p}}} [\zeta_{\mathrm{p}} - \tilde{\zeta}_{\mathrm{p}}(hp_{1-3}(i))]^2} \\ \text{s.t.} \quad & \text{Eqs. (12)-(13)} \\ & hp_{\min} \le hp_{1-3} \le hp_{\max} \end{aligned} \tag{14}$$

where ζ_{p} and $\hat{\zeta}_{\mathrm{p}}$ denote the prediction dataset and the correspondingly estimated values, respectively.

4. OPTIMAL DESIGN OF THE OPERATING CONDITIONS

To facilitate quality-by-design (QbD) of seeded cooling crystallization process operation, an optimal input design is proposed herein to achieve high quality crystal products with narrow CSD with regard to the target mean crystal size, based on the above surrogate modeling.

In view of that the information entropy in Eq.(8) is a common index to evaluate the flatness or sharpness of a distribution curve, it is adopted herein to assess the concentration degree of product CSD. Note that the desired sizes of crystal products are generally in a range of the target size in practice, rather than only the target size. It is therefore proposed to define a ratio of the desired crystal product yield with regards to the target crystal size over the total crystal products, i.e.,

$$A = \int_{90\%DS}^{110\%DS} \zeta(\boldsymbol{o}, y_{n_k}) \, \mathrm{dL} \Big/ \int_{0}^{+\infty} \zeta(\boldsymbol{o}, y_{n_k}) \mathrm{dL} \tag{15}$$

where DS denotes the desired product crystal size.

Taking into account the above information entropy in (8) and ratio in (15) for assessing crystal product quality, a comprehensive criterion is therefore proposed as

$$Q = \Omega + w_{\mathrm{q}}(1/A) \tag{16}$$

where w_{q} is a coefficient factor for scaling.

Hence, the above operating conditions are optimized by minimizing Q in (16), i.e.,

$$\min_{T(t)} \ \boldsymbol{Q}$$
$$\text{s.t.} \quad \text{Eqs. (12)-(13)} \qquad (17)$$
$$\boldsymbol{CR}_{\min} \le \boldsymbol{CR} \le \boldsymbol{CR}_{\max}$$
$$\boldsymbol{SS}_{\min} \le \boldsymbol{SS} \le \boldsymbol{SS}_{\max}$$

where $CR_{\min}$ and $CR_{\max}$ indicate the lower and upper bounds of cooling rate, respectively; $SS_{\min}$ and $SS_{\max}$ denote the lower and upper bounds of initial solution supersaturation, respectively.

5. CASE STUDY ON LGA COOLING CRYSTALLIZATION PROCESS

A number of seeded β form LGA cooling crystallization experiments were performed based on the experimental setup shown in Figure 2.

The crystallizer consists of a 1L jacketed glass reactor, a thermostatic circulator (made by Julabo company), and a PTFE four-paddle agitator. The chord length distribution (CLD) of crystals is measured by a focused beam reflectance measurement (FBRM) instrument (Mettler-Toledo company). The solution concentration is measured by the attenuated total internal reflection-Fourier transform infrared (ATR-FTIR) spectroscopy (Mettler-Toledo company).

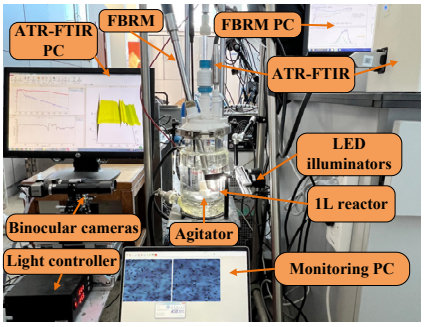

Figure 2. Experimental set-up for LGA crystallization

In this study, the solute is taken as the β-LGA crystals with a purity of 99%, and the solvent is distilled water. In each experiment, the batch time of each experiment was taken as 90 minutes. The initial solution supersaturation were set as 1.0, 1.1, 1.2, and 1.3 along with the linear cooling rates of 0.1, 0.2, 0.3, and 0.4 °C/min for each batch experiment.

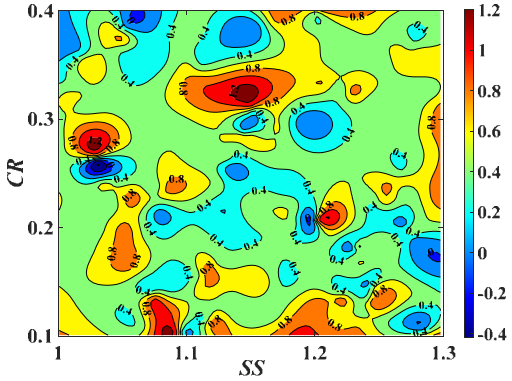

Figure 3. Sensitivity plot of product CSD with regard to the operating conditions based on initial GPR model

It is seen in Figure 3 that the information entropy of product CSD defined in Eq.(8), from which high sensitivity ($S_{CR,SS} > \Delta$) could be found around R-1, 3, 4, 5, 7, 9, 10, 12, 14, 15, and 16. Hence, a sensitivity threshold $\Delta = 0.4$ is taken for selecting the operating conditions to generate batch run data for surrogate modeling. The selection result is listed in Table 1.

Table 1. Batch run design by SDoE for surrogate modelling

CR / *SS*	1.0	1.1	1.2	1.3
0.1	R-1	/	R-3	R-4
0.2	R-5	/	R-7	/
0.3	R-9	R-10	/	R-12
0.4	R-13	R-14	R-15	R-16

For clarity, the FFD and SDoE for β-LGA crystallization under the permitted range of operating conditions are indicated in Figure 1. To assess the performance of constructed models, the R^2 defined below are used,

$$R^2 = 1 - \frac{(\zeta - \hat{\zeta})^{\mathrm{T}}(\zeta - \hat{\zeta})}{(\zeta - \bar{\zeta})^{\mathrm{T}}(\zeta - \bar{\zeta})} \qquad (18)$$

where $\hat{\zeta}$ is the predicted CSD in each experiment, and $\bar{\zeta}$ is the mean vector.

Table 2. Comparison of R^2 and RMSE indices for GPR modeling by MLE and BWO

Optimized by **MLE**		
GPR modeling	R^2	RMSE
FFD	0.992	$5.59e^{-4}$
SDoE	0.997	**$4.14e^{-4}$**
Optimized by **BWO**		
FFD	0.999	$2.58e^{-4}$
SDoE	0.999	**$2.15e^{-4}$**

It is seen that the hyperparameters setting of GPR model optimized by BWO could obtain better prediction results in comparison with MLE, as listed in Table 2.

The proposed GPR model and the recently developed double-layer (DL) modeling method (Song et al., 2022) are applied for comparison. Based on the product CSD measured by microscopy and the operating conditions of *CR* and *SS* listed in Table 1, a prediction model of product CSD is built by the proposed surrogate modeling method.

It is seen in Figure 4 that the product CSD (solid black line) is effectively fitted by the GPR models built by FFD (dash line) and SDoE (dot line), in comparison with the recently developed DL modeling method.

To demonstrate the effectiveness of the proposed method, Figure 5 shows the prediction results of product CSD by using the GPR model built by SDoE under additional batch run named R-11. It can be found that both GPR models built by FFD and SDoE could evidently improve prediction accuracy

on the product CSD, compared with the DL modeling method.

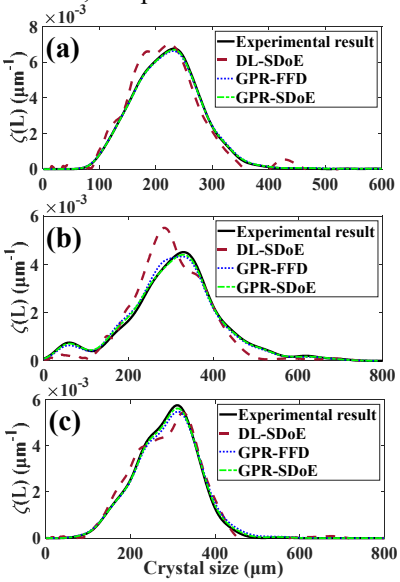

Figure 4. Fitting results by different modeling methods based on FFD and SDoE: (a) R-4; (b) R-7; (c) R-13

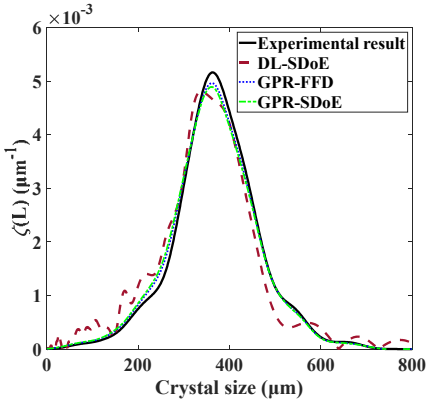

Figure 5. Prediction results of product CSD by different modeling methods under R-11 for verification

To maximize the product yield and enhance the concentration of product CSD around the desired crystal size of $350\mu m$, the optimal cooling rate and initial solution supersaturation are determined as CR=0.39 (℃/min) and SS=1.06 by the above GPR modeling with SDoE, corresponding to Q_1=8.3349 and A_1=33.36%. In contrast, the optimal operating conditions are determined as CR=0.34 (℃/min) and SS=1.21 for GPR modeling with FFD, corresponding to Q_2=8.5743 and A_2=27.04%. Similarly, they are determined as CR=0.26 (℃/min) and SS=1.06 by the DL modeling with the above SDoE, corresponding to Q_3=9.1328 and A_3=28.35%.

Figure 6 shows that the optimized CSD based on FFD and SDoE are more concentrated around the target size of $350\mu m$, compared with the previous DL modeling and optimization method based on the proposed SDoE. Moreover, the proposed optimization method based on the SDoE for GPR modeling acquires evidently higher product yield in the desired product crystal size range, compared with that of FFD.

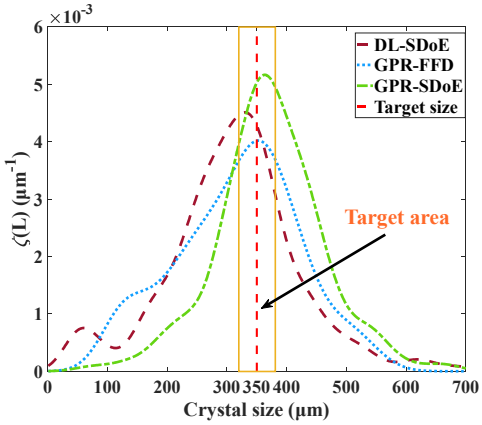

Figure 6. Experimental verification of the optimized product CSDs by different modeling methods

Table 3 lists the crystal product yields in (15) by different methods, which indicates that the proposed method obviously enhances the concentration of product CSD as well as the product yield around the desired product size. Note that the product crystal yield by SDoE in the desired size range of [90,110]%×350 μm is over 12% higher than that of FFD based on the same optimization method, and almost 30% higher than the previous DL modeling and optimization method.

Table 3 Comparison of crystal product yields by different modeling methods

	DL-SDoE	GPR-FFD	GPR-SDoE
Yield	28.35%	27.04%	**33.36%**

Figure 7 shows the microscopic images of crystal products with a mean length of $350\mu m$ acquired by the proposed optimization method based on SDoE and FFD, respectively, along with the previous DL modeling and optimization method (Song et al., 2022). It can be seen that needle-like β-form LGA crystals with a higher aspect ratio are obtained by the proposed optimization method based on SDoE, and meanwhile, fine crystals are apparently reduced in the products.

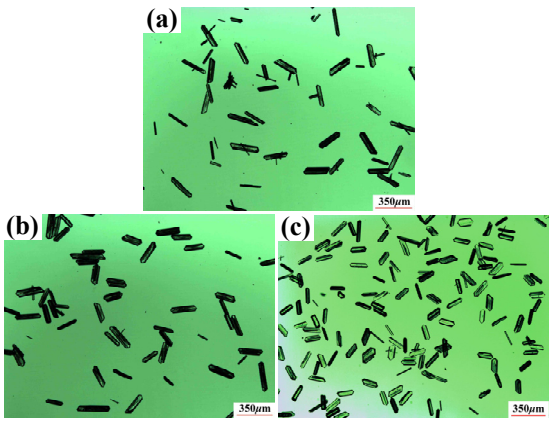

Figure 7. Microscopic view of the optimal experimental results: (a) DL-SDoE; (b) GPR-FFD; (c) GPR-SDoE

6. CONCLUSIONS

A GPR based surrogate modelling method has been proposed in this paper to reflect the nonlinear mapping relationship between the operating conditions of β form LGA seeded cooling crystallization and product CSD. A modified DoE has been presented to save the number of real experiments for building up the surrogate model, which could obtain similar or even better performance on predicting the product CSD than that of FFD. Moreover, a comprehensive quality criterion that combines the information entropy of product CSD with the desired product crystal size range has been introduced for the optimization of operating conditions, which could effectively enhance the concentration of product CSD along with the product yield in the target crystal size range. Experiments on seeded β form LGA crystallization verified that the optimized operating conditions by the proposed SDoE and GPR model could evidently improve the concentration of product CSD together with the product yield with regard to the target crystal size, in comparison with the traditional DoE of FFD and a recent DL modelling method for the optimal input design.

ACKNOWLEDGMENT

This work is supported in part by the NSF China Grants 62173058, 62361136585 and 62327807.

REFERENCES

Aamir, E., Nagy, Z. K., Rielly, C. D., Kleinert, T., & Judat, B. (2009). Combined quadrature method of moments and method of characteristics approach for efficient solution of population balance models for dynamic modeling and crystal size distribution control of crystallization processes. Ind. Eng. Chem. Res., 48(18), 8575-8584.

Busschaert, M., & Waldherr, S. (2022). Inference of kinetics in population balance models using Gaussian process regression. IFAC-PapersOnLine, 55(7), 384-391.

Deringer, V. L., Bartók, A. P., Bernstein, N., Wilkins, D. M., Ceriotti, M., & Csányi, G. (2021). Gaussian process regression for materials and molecules. Chem. Rev., 121(16), 10073-10141.

Gimbun, J., Nagy, Z. K., & Rielly, C. D. (2009). Simultaneous quadrature method of moments for the solution of population balance equations, using a differential algebraic equation framework. Ind. Eng. Chem. Res., 48(16), 7798-7812.

Gunawan, R., Fusman, I., & Braatz, R. D. (2004). High resolution algorithms for multidimensional population balance equations. AlChE J., 50(11), 2738-2749.

Hemalatha, K., & Rani, K. Y. (2017). Multiobjective optimization of unseeded and seeded batch cooling crystallization processes. Ind. Eng. Chem. Res., 56(20), 6012-6021.

Hermanto, M. W., Kee, N. C., Tan, R. B. H., Chiu, M.-S., & Braatz, R. D. (2008). Robust Bayesian estimation of kinetics for the polymorphic transformation of L-glutamic acid crystals. AlChE J., 54(12), 3248-3259.

Khan, S., Ma, C. Y., Mahmud, T., Penchev, R. Y., Roberts, K. J., Morris, J., Özkan, L., White, G., Grieve, B., Hall, A., Buser, P., Gibson, N., Keller, P., Shuttleworth, P., & Price, C. J. (2011). In-process monitoring and control of supersaturation in seeded batch cooling crystallisation of L-glutamic acid: From laboratory to industrial pilot plant. Org. Process Res. Dev., 15(3), 540-555.

Ljungberg, F., Linder, J., Enqvist, M., & Tervo, K. (2023). Dictionary-based experiment design for estimation of marine models. Control Eng. Pract., 135, 105528.

Montgomery, D. C. Design and analysis of experiments. The 2^k factorial design. John wiley & sons; 2017. p. 230-253.

Nagy, Z. K., Fevotte, G., Kramer, H., & Simon, L. L. (2013). Recent advances in the monitoring, modelling and control of crystallization systems. Chem. Eng. Res. Des., 91(10), 1903-1922.

Saltelli, A., Annoni, P., Azzini, I., Campolongo, F., Ratto, M., & Tarantola, S. (2010). Variance based sensitivity analysis of model output. Design and estimator for the total sensitivity index. Comput. Phys. Commun., 181(2), 259-270.

Sanzida, N., & Nagy, Z. K. (2014). Polynomial chaos expansion (PCE) based surrogate modeling and optimization for batch crystallization processes. Comput.-Aided Chem. Eng., 33, 565-570.

Seki, H., & Su, Y. (2015). Robust optimal temperature swing operations for size control of seeded batch cooling crystallization. Chem. Eng. Sci., 133, 16-23.

Simone, E., Szilagyi, B., & Nagy, Z. K. (2017). Systematic model identification and optimization-based active polymorphic control of crystallization processes. Chem. Eng. Sci., 174, 374-386.

Song, B., Liu, T., Yang, S., Liu, J., & Chen, J. (2022). Data-driven operation modeling and optimal design for batch cooling crystallization with a case study on β-LGA. Ind. Eng. Chem. Res., 61(51), 18795-18809.

Williams, C. K., & Rasmussen, C. E. Gaussian processes for machine learning. MIT press Cambridge, MA; 2006.

Zhong, C., Li, G., & Meng, Z. (2022). Beluga whale optimization: A novel nature-inspired metaheuristic algorithm. Knowl-Based Syst, 251, 109215.

Zhong, W., Qiao, C., Peng, X., Li, Z., Fan, C., & Qian, F. (2019). Operation optimization of hydrocracking process based on kriging surrogate model. Control Eng. Pract., 85, 34-40.